

## Optical BPSK Subcarrier Modulation Using an Integrated Hybrid Device

M. Shin<sup>1)</sup>, J. Lim<sup>1)</sup>, J. Kim<sup>2)</sup>, J. S. Kim<sup>2)</sup>, K. E. Pyun<sup>2)</sup>, and S. Hong<sup>1)</sup>

<sup>1)</sup> Department of Electrical Engineering, KAIST, 373-1 Kusong-Dong, Yusong-Gu, Taejon 305-701, South Korea

Tel: +82-42-869-8049, Fax: +82-42-869-8560 e-mail address: mhshin@cais.kaist.ac.kr

<sup>2)</sup> Telecommunication Basic Research Lab., ETRI, Yusong PO Box 106, Taejon 305-600, South Korea

### 1. Introduction

Microwave and millimeter (mm) wave via a fiber are receiving increasing attention since hybrid fiber/coax network allows robust transmission of RF subcarrier and thus the significant reduction in the number of cascade RF amplifiers. The digital transmission systems with microwave and mm wave using QPSK or BPSK modulation have been reported [1] [2]. Although mm wave subcarrier bands have the capacity of higher than 1 Gb/s, most of previous works reported at most a few hundred Mb/s. This is because up-conversion schemes in the transmitter use an intermediate frequency to convert base band signal to mm-wave band, and as a result, the data rate cannot exceed the intermediate frequency. Also are needed high frequency amplifiers and mixers that are very difficult to implement if one wants to utilize the full capacity of mm-wave carriers.

We had presented the modulation principle of an integrated hybrid device at low frequency region [3]. This utilizes the interference of multimode interference (MMI) coupler as well as the optical amplitude modulation of modulators. In this paper, the BPSK modulation of 10 GHz subcarrier is presented. Also are measured the bandwidth of the device and the spectrum of the modulated optical signal.

### 2. Device and Fabrication

The device structure is illustrated in Fig. 1. The input 3dB MMI coupler divides and branches an incident light to two equal MQW EA modulators. The MMI coupler is designed to have a mirror image at an output using paired interference [4]. Thus, two optical outputs of the MMI coupler have the same amplitude but  $\pi/2$  phase difference. Since these input/output MMI couplers, which are designed to be the same, are connected to the optical modulators, the output of the device has out-of-phase image of which the optical fields interfere destructively. The optical amplitude of the signal in each branch is varied when it pass through the EA modulators. If the modulator  $M_1$  is turned off, the optical amplitude at the output is directly proportional to that through the modulator  $M_2$ . If the modulator  $M_1$  is turned on, the optical amplitude at the output is related to the difference of the optical amplitudes through both modulator  $M_1$  and  $M_2$ .

If it is assumed that the modulator  $M_1$  and  $M_2$  are identical and a digital on-and-off signal (0 or 1) is applied to the modulator  $M_1$  while a sinusoidal signal of amplitude  $m_2$

and frequency  $\omega$  is applied to the modulator  $M_2$ , then the optical amplitude at the output can be written in (1).

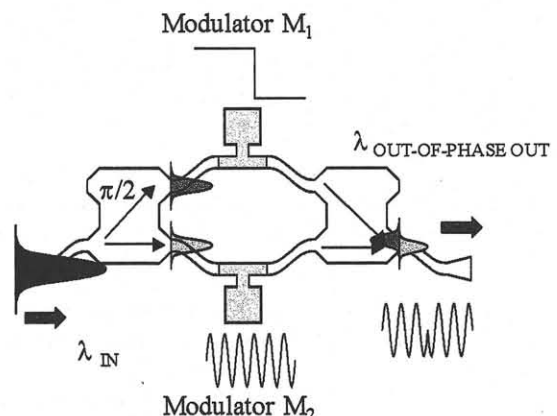


Fig. 1 The integrated device configuration. The optical phase is different by  $\pi$  at the out-of-phase output port

$$P_{out-of-phase} = \begin{cases} A_0 [1 - m_2 \sin(\omega t)] & \text{if } M_1 \text{ is turned ON} \\ A_0 [1 + m_2 \sin(\omega t)] & \text{if } M_1 \text{ is turned OFF} \end{cases} \quad (1)$$

$$= A_0 [1 + m_2 \sin(\omega t + \pi(M_1))]$$

where  $A_0$  is maximum optical power at the output port.

Note that the sign of the amplitude  $m_2$  is changed so that the phase of sinusoidal signal generated at the modulator  $M_2$  is shifted by  $\pi$  in accordance with the state of the modulator  $M_1$ . Since the subcarrier and the digital data are introduced independently to the modulators, the subcarrier frequency and the data rate are limited only by the bandwidth of high-speed EA modulators. Therefore, the direct up-conversion from base band to mm-wave band is possible.

The proposed device was fabricated in the following process. The epitaxial layers of the modulator region were prepared on  $n^+$ -InP substrate by using a metal organic chemical vapor deposition (MOCVD). The multiple quantum well (MQW) absorption layers of 250 nm thickness were grown between graded index clads of 70 nm thickness. The low loss passive region was grown by butt-coupled regrowth. Deep dry etching was applied to form the waveguide structures including MMI couplers and MQW EA modulators. A 3  $\mu\text{m}$ -thick polyimide was employed to block the leakage current and to reduce the pad

capacitance [3].

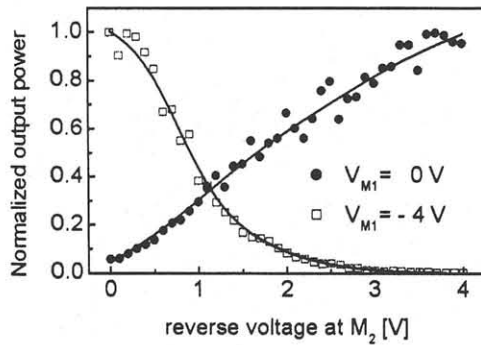


Fig. 2 Normalized output power at the out-of-phase port as a function of the applied carrier signal voltage.

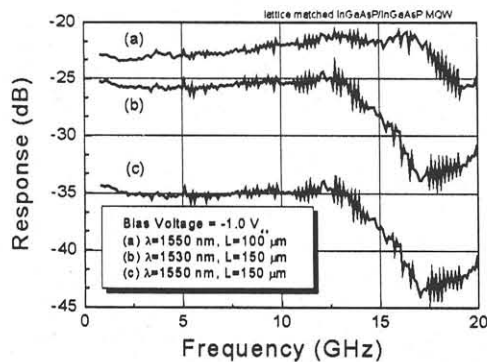


Fig. 3 Small signal frequency response of the MQW EA modulator.

### 3. Measurement results

The characteristics of MMI couplers and EA modulators strongly depend on the wavelength and polarization of light. We used an HP8168F tunable laser and controlled the polarization with a three-paddle fiber rotating polarizer. These adjustments were monitored using an IR-Vidicon CCD camera. A  $1.53 \mu\text{m}$  light of TE mode was selected to operate the MMI couplers in the optimum condition and to have a large on-off ratio of the modulators. The incident power of light was set at 5 mW. Each modulator was turned off when a reverse voltage of 4 V is applied. When the voltage of -4 V was applied to the modulator  $M_1$  (OFF state), the out-of-phase output was decreased as the reverse voltage was increased to  $M_2$ . On the contrary, when  $M_1$  was biased with 0 V (ON state), the output was increased with the reverse voltage at  $M_2$ . This is because when  $M_1$  is on, the difference between the optical outputs from two modulators, which appears at the output, increases as  $M_2$  becomes opaque. We measured the over all modulation characteristics by using an optical power detector. Fig. 2 shows that the bias voltage of  $M_1$  changes the sign of the optical signal modulated with the reverse voltage of  $M_2$ . The phase of output signal was then changed by  $\pi$  in comparison with that of input signal.

As for the EA modulator, we measured the optical and electrical properties of the EA modulators in this device. The on-off ratio at -3 V was 16 dB for TE mode and 13 dB

for TM mode at  $1.53 \mu\text{m}$  wavelength. The 3 dB bandwidth of the modulators was 18 GHz as shown in Fig. 3. An RF signal of 10 GHz with 5 dBm to the  $M_2$  modulator was driven and a 4 V 10 MHz rectangular pulse train to  $M_1$  was driven directly as a base band digital signal. We compared the output signal spectrum from the photodiode because it was not easy to confirm the phase change of the high-frequency signals. The output spectrum detected by a photodiode was shown in Fig. 4. Since the phase of the carrier frequency was changed by  $\pi$  periodically, along with the pulse train signal, the power at the carrier frequency (center frequency of 10 GHz) disappeared, which is unique difference from the sinc-function-like spectrum of the pulse train.

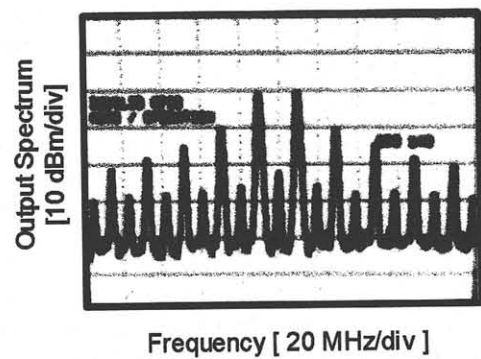


Fig. 4 Spectrum response of the modulated output near the center frequency

### 4. Conclusions

Base band signal had been directly up-converted to the 10 GHz RF subcarrier using the optical/RF hybrid device. Since the carrier frequency and the data rate are expected to be limited only by the bandwidth of modulator, one can readily extend this operation principle to the mm-wave subcarrier and the data rate of its full bandwidth capacity. In addition, the synchronization of local oscillator for RF subcarrier and digital signal is not necessary in this scheme. This is because, in this modulation, the signal phase can be changed at arbitrary time by optical interference.

### Acknowledgements

This work was partially supported by the Ministry of Information and Communications at ETRI.

### References

- [1] L. Noel, D. Wake, D. G. Moodie, D. D. Marcenac, L. D. Westbrook, and D. Nesset, *IEEE Trans. Microwave Theory & Techniq.*, vol. 45, pp.1416-1422, Aug. 1997.
- [2] T. K. Woodward, S. Hunsche, A. J. Ritger, and J. B. Stark, *IEEE Photon. Technol. Lett.*, vol. 11, pp. 382-384, Mar. 1999.
- [3] M. Shin, J. Lim, C. Y. Park, J. Kim, J. S. Kim, K. E. Pyun, and S. Hong, in *Tech. Dig., International Topical Meeting on MWP'99*, Melbourne, Australia, Nov. 1999, paper T-8.4.
- [4] L. B. Soldano, and C. M. Pennings, *J. Lightwave Technol.*, vol. 13, pp. 615-627, Apr. 1995.